# The MGB-IPH model for large-scale rainfall–runoff modelling

**WALTER COLLISCHONN, DANIEL ALLASIA, BENEDITO C. DA SILVA & CARLOS E. M. TUCCI**

*Instituto de Pesquisas Hidráulicas, Universidade Federal do Rio Grande do Sul, Av. Bento Gonçalves, 9500 CEP 91501-970, Caixa Postal 15029, Porto Alegre RS, Brazil*

collischonn@iph.ufrgs.br

**Abstract** Recent developments in hydrological modelling of river basins are focused on prediction in ungauged basins, which implies the need to improve relationships between model parameters and easily-obtainable information, such as satellite images, and to test the transferability of model parameters. A large-scale distributed hydrological model is described, which has been used in several large river basins in Brazil. The model parameters are related to classes of physical characteristics, such as soil type, land use, geology and vegetation. The model uses two basin space units: square grids for flow direction along the basin and GRU—group response units—which are hydrological classes of the basin physical characteristics for water balance. Expected ranges of parameter values are associated with each of these classes during the model calibration. Results are presented of the model fitting in the Taquari-Antas River basin in Brazil (26 000 km$^2$ and 11 flow gauges). Based on this fitting, the model was then applied to the Upper Uruguay River basin (52 000 km$^2$), having similar physical conditions, without any further calibration, in order to test the transferability of the model. The results in the Uruguay basin were compared with recorded flow data and showed relatively small errors, although a tendency to underestimate mean flows was found.

**Key words** South America; River Uruguay; River Taquari; hydrological model; large basins; ungauged basins; parameter fitting

## Le modèle MGB–IPH pour la modélisation pluie–débit à grande échelle

**Résumé** De récents développements en modélisation hydrologique de bassins versants sont centrés sur la prévision en bassins non jaugés, ce qui nécessite d'améliorer les relations entre les paramètres du modèle et les informations facilement accessibles, comme les images satellitales, et de tester la tranférabilité des paramètres de modélisation. Cet article décrit un modèle hydrologique distribué à grande échelle, qui a déjà été utilisé pour plusieurs grands bassins versants au Brésil. Les paramètres du modèle sont liés à des classes de caractéristiques physiques, telles que le type de sol, l'occupation du sol, la géologie et la végétation. Le modèle s'appuie sur deux unités spatiales: des mailles carrées pour les directions d'écoulement à travers le bassin et des UGR—unités groupées de réponse—qui sont des classes de caractéristiques physiques du bassin vis à vis du bilan hydrologique. Les gammes attendues des valeurs des paramètres sont associées à chacune de ces classes lors du calage du modèle. Les résultats du calage du modèle pour le bassin Brésilien de la Rivière Taquari-Antas (26 000 km² et 11 stations de jaugeage) sont présentés. Puis, à partir de ce calage, le modèle a été appliqué au bassin du cours supérieur de la Rivière Uruguay (52 000 km²), qui présente des conditions similaires, sans aucun calage supplémentaire, afin de tester la transférabilité du modèle. Les résultats dans le bassin de l'Uruguay ont été comparés avec des données de débit observées et des erreurs relativement faibles ont été mises en évidence, malgré une tendance à la sous-estimation des débits moyens.

**Mots clefs** Amérique du sud; Rivière Uruguay; Rivière Taquari; modèle hydrologique; grands bassins versants; bassins versant non jaugés; ajustement des paramètres

## INTRODUCTION

Large-scale hydrological modelling in basins with scarce data is needed to address several problems in water resources management. This is especially true in the case of South American countries, where some of world's largest basins lie in regions covered by sparse networks of rainfall and flow gauges, and where maps are usually available at relatively low resolution.

From a historical point of view, the interest in large-scale hydrological models stems from the need to have modelling tools for the land phase of the hydrological cycle in global circulation models (Sausen *et al*., 1994; Wood *et al*., 1992; Evans,

 

2003), and also because of the need to manage international conflicts related to water in transboundary basins (Andersen *et al*., 2001). Models are also needed for hydrological forecasting (Bremicker *et al.*, 2004), to assess the effects of widespread land cover change on streamflow (Matheussen *et al*., 2000), and to estimate climate change effects on streamflow (Guo *et al*., 2002).

There are several examples of macro-scale hydrological models developed in the last years (Singh & Frevert, 2002), including: the VIC family of models (Wood *et al*., 1992; Liang *et al*., 1994); ISBA-MODCOU (Habets *et al*., 1999); WATFLOOD (Kouwen & Mousavi, 2002; Soulis *et al*., 2004); LARSIM (Ludwig & Bremicker, 2006); and SWIM (Krysanova *et al*., 1998). Other distributed models, such as SHE (Refsgaard & Storm, 1995), originally developed as a small-scale model, have been also applied at larger scales than originally intended (Andersen *et al*., 2001).

Most of those models assume that a relationship exists between the values of the model parameters and characteristics that could be measured or classified over the basin, such as soils, vegetation and topography (Kite & Kouwen, 1992; Habets *et al.*, 1999). This assumption can be understood as an advance in the search for hydrological models that could be applied without calibration, as proposed in the PUB scientific plan (Sivapalan *et al*., 2003), or as an attempt to reduce the number of parameters that need to be calibrated, thereby reducing the degrees of freedom of the calibration process (Beven, 2001a; Andersen *et al.*, 2001).

The basic assumption is that associations can be established which relate readily available data to model parameter values. This assumption should be tested for geographical transferability, at least by a proxy-basin test (Klemes, 1986), using data of two basins with similar characteristics.

With a focus on large South American basins, and bearing in mind the typical low spatial density and limited duration of hydrological records available in the region, a large-scale distributed hydrological model has been developed, named MGB-IPH (an acronym from the Portuguese for Large Basins Model and Institute of Hydraulic Research) in which land use, topography, vegetation cover and soil types are used as guides to select parameter values. The MGB-IPH model was initially based on the LARSIM (Ludwig & Bremicker, 2006) and VIC (Liang *et al*., 1994; Nijssem *et al*., 1997) models, with some changes to the evapotranspiration, percolation and channel-routing modules. Applications of this model were initially developed for Brazilian basins (Collischonn & Tucci, 2001), but, in recent years, the model has been tested and used in other South American basins (Fig. 1) from the sub-tropical, rapid-response basins of southern Brazil and Uruguay, to the Pantanal region lying between Bolivia and Brazil, where drainage basins are marked by seasonal rainfall and, in some cases, slow response hydrographs. Other applications of the MGB-IPH model include: the São Francisco River basin (640 000 km$^2$), which lies partly in the semi-arid region of Northeast Brazil (Tucci *et al*., 2005); the Madeira River, one of the most important tributaries of the Amazon (Ribeiro *et al*., 2005); and the Tapajos River, another tributary of the Amazon, where satellite-derived rainfall information is being used to run the model. The main aspects of those applications have been described by Allasia *et al.* (2006).

This paper describes the MGB-IPH model and reports the results of a proxy basin test in which transferability of the model parameters was evaluated. This test aimed to check the validity of the association between readily available data (soils, vegetation cover and topography) and parameter values. The model was fitted and verified for the


**Fig. 1** South American basins where the large-scale MGB-IPH model has been applied (Allasia *et al*., 2006).

Taquari-Antas River basin (about 26 000 km$^2$ in area) in southern Brazil, with 11 flow gauges and 11 years of rainfall and streamflow data. It was then applied to the nearby Upper Uruguay River basin (52 671 km$^2$), using the same relationship between parameter values and soil type classes, land use and vegetation cover as was found in the Taquari-Antas River basin, as if the Uruguay basin were ungauged.

## THE LARGE-BASIN DISTRIBUTED HYDROLOGICAL MODEL MGB-IPH

The MGB-IPH model is composed of modules for the calculation of soil water budget, evapotranspiration, flow propagation within a cell, and flow routing through the drainage network. The drainage basin is divided into elements of area (normally square grids or cells) interconnected by channels, with vegetation and land use within each element categorized into one or more classes. The grouped response unit (GRU) (Kouwen *et al*., 1993), or hydrological response unit (Beven, 2001b) approach is used for hydrological classification of all areas with a similar combination of soil and land cover, irrespective of its location within the cell (Fig. 2).

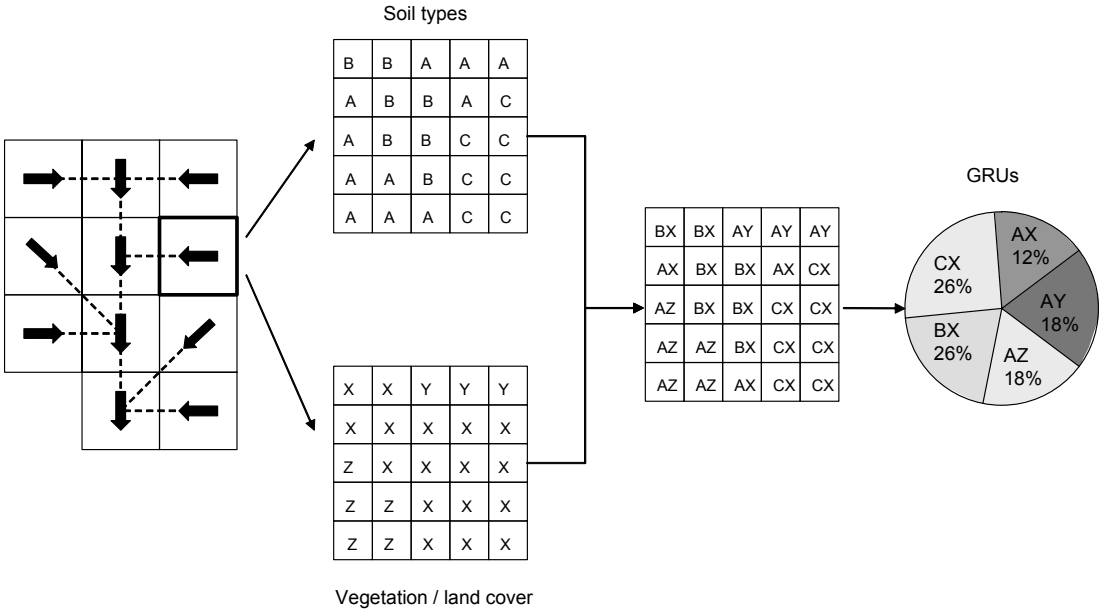


**Fig. 2** Basin discretization in square cells and the grouped response unit concept (adapted from Kouwen & Mousavi, 2002).

A cell contains a limited number of distinct GRUs. Soil water budget is computed for each GRU, and runoff generated from the different GRUs in the cell is then summed and routed to the stream channel and routed further through the river network. This approach has been used in several large-scale hydrological models, such as VIC (Wood *et al*., 1992; Liang *et al*., 1994; Nijssem *et al*., 1997) and WATFLOOD (Kouwen & Mousavi, 2002; Soulis *et al*., 2004).

Soil water balance is computed independently for each GRU of each cell, considering only one soil layer, according to equation (1) (see Fig. 3):

$$W_{i,j}^{k} = W_{i,j}^{k-1} + \left(P_i - ET_{i,j} - D\sup_{i,j} - D\mathrm{int}_{i,j} - D\mathrm{bas}_{i,j}\right)\Delta t \quad (1)$$

where $k$, $i$ and $j$ are indexes related to time step, cell and GRU, respectively; $\Delta t$ is the

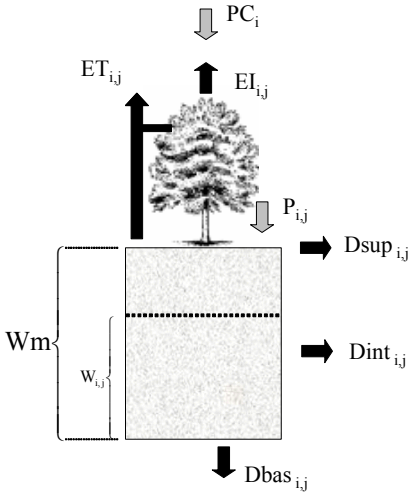


**Fig. 3** Schematic of the soil water budget in each GRU of a cell.

time step (1 day in most applications); $W_{i,j}^{k}$ (mm) is the water storage in the soil layer, at the end of the $k$th time step, of the $j$th GRU of the $i$th cell; $W_{i,j}^{k-1}$ (mm) is the same variable at the start of the time step; $P_{i,j}$ (mm $\Delta t^{-1}$) is the rainfall that reaches the soil; $ET_{i,j}$ (mm $\Delta t^{-1}$) is the evapotranspiration from the soil; $D\text{sup}_{i,j}$ (mm $\Delta t^{-1}$) is the surface runoff, or quick flow; $D\text{int}_{i,j}$ (mm $\Delta t^{-1}$) is the subsurface flow; $D\text{bas}_{i,j}$ (mm $\Delta t^{-1}$) is the flow to the groundwater reservoir. Variables $W_{i,j}^{k}$ and $P_{i,j}$ are known in each time step, and $ET_{i,j}$, $D\text{sup}_{i,j}$, $D\text{int}_{i,j}$ and $D\text{bas}_{i,j}$ are calculated based on soil water storage at the start of the time step ($W_{i,j}^{k}$) and on model parameters, according to the following:

$$D\text{sup}_{i,j} = \Delta t \cdot P_i - \left(W\text{m}_j - W_{i,j}^{k-1}\right) \qquad \text{for } A \le 0 \tag{2a}$$

$$D\text{sup}_{i,j} = \Delta t \cdot P_i - \left(W\text{m}_j - W_{i,j}^{k-1}\right) + W\text{m}_j \left[ \left( 1 - \frac{W_{i,j}^{k-1}}{W\text{m}_j} \right)^{\frac{1}{b_j+1}} - \frac{\Delta t \cdot P_i}{W\text{m}_j \left(b_j + 1\right)} \right]^{b_j+1} \qquad \text{for } y > 0 \tag{2b}$$

where $y = \left[ \left( 1 - \frac{W_{i,j}^{k-1}}{W\text{m}_j} \right)^{\frac{1}{b_j+1}} - \frac{\Delta t \cdot P_i}{\left(b_j + 1\right) W\text{m}_j} \right]$

and where $W\text{m}_j$ (mm) is maximum water storage in the upper layer of soil of GRU $j$ (GRU related parameter); $b_j$ [-] is the GRU related parameter, explained below.

Equation (2) is based on the variable contributing area concept of the Arno (Todini, 1996), Xinanjiang (Zhao *et al.*, 1980), VIC (Liang *et al.*, 1994) and LARSIM (Ludwig & Bremicker, 2006) models. The parameter $b_j$ [-] represents the statistical distribution of water storage capacity of the soil. If $b_j$ is set to zero, then the whole area covered by a particular GRU will have a storage capacity of $W\text{m}_j$ (mm) in the upper layer of soil. For positive values of $b_j$, some portions of the GRU area will have soil storage capacity lower than $W\text{m}_j$, thus originating more runoff, even for minor rainfall events. A complete description of this formulation can be found in Todini (1996).

Subsurface flow is obtained using a function similar to the Brooks and Corey non-saturated hydraulic conductivity equation (Rawls *et al.*, 1993):

$$D\text{int}_{i,j} = K\text{int}_j \left( \frac{W_{i,j} - W\text{z}_j}{W\text{m}_j - W\text{z}_j} \right)^{\left(3 + 2/\lambda_j\right)} \tag{3}$$

where $W\text{z}_j$ (mm) is the lower limit below which there is no subsurface flow; $K\text{int}_j$ (mm $\Delta t^{-1}$) is a parameter which gives the subsurface drainage of the water from the soil layer, when the soil is saturated; and $\lambda$ [-] is the soil porosity index.

Percolation from the soil layer to groundwater is calculated according to a linear relationship between soil water storage and maximum soil water storage:

$$D\text{bas}_{i,j} = K\text{bas}_j \cdot \frac{\left(W_{i,j}^{k-1} - W\text{c}_j\right)}{\left(W\text{m}_j - W\text{c}_j\right)} \tag{4}$$

where $W\text{c}_j$ (mm) is the lower limit below which there is no flow; and $K\text{bas}_j$ (mm $\Delta t^{-1}$)

is a parameter which gives the percolation rate to groundwater in the case of saturated soil.

Evapotranspiration from soil, vegetation and canopy to the atmosphere is estimated by the Penman-Monteith equation (equation (5)), using an approach similar to that of Wigmosta *et al*. (1994). Meteorological conditions (air temperature, solar radiation, wind speed, precipitation, relative humidity and atmospheric pressure) are prescribed for each grid cell based on interpolation of nearby measurement stations. Evaporation can occur from the interception storage (evaporation) and from the soil (directly or through transpiration of the plants—evapotranspiration).

$$e = \left( \frac{\Delta \cdot A + \rho_A \cdot c_p \cdot \dfrac{D}{r_a}}{\Delta + \gamma\left(1 + \dfrac{r_s}{r_a}\right)} \right) \frac{1}{\lambda \cdot \rho_W} \tag{5}$$

where $e$ (m s$^{-1}$) is the evaporation or evapotranspiration flux, $\lambda$ (MJ kg$^{-1}$) is the latent heat of vaporization, $\Delta$ (kPa ºC$^{-1}$) is the gradient of the saturated vapour pressure–temperature function, $A$ (MJ m$^{-2}$ s$^{-1}$) is the available energy, $\rho_A$ (kg m$^{-3}$) is the density of air, $\rho_W$ (kg m$^{-3}$) is the specific mass of water, $c_p$ (MJ kg$^{-1}$ ºC$^{-1}$) is the specific heat of moist air, $D$ (kPa) is the vapour pressure deficit, $\gamma$ (kPa ºC$^{-1}$) is the psychrometric constant, $r_s$ (s m$^{-1}$) is the surface resistance of the land cover and $r_a$ (s m$^{-1}$) is the aerodynamic resistance.

Precipitation is assumed to be stored on the surface of the vegetation until maximum interception storage capacity is reached, which is determined for each GRU based on the leaf area index (LAI), according to equation (6).

$$S\max_j = \alpha \cdot \mathrm{LAI}_{j,m} \tag{6}$$

where $S\max_j$ is the maximum interception storage capacity for GRU $j$, and $\alpha$ is a parameter assumed to have a fixed value of 0.2 mm (Ubarana, 1996). The $\mathrm{LAI}_{j,m}$ values are obtained from the literature and may have a seasonal variation, with different values for each month of the year (m).

Changes in interception storage are calculated in two stages for each time step. Initially the interception storage receives water from rainfall (equation (7)), and only the excess precipitation (throughfall) passes through the canopy to reach the soil surface (equation (8)). Subsequently, intercepted water is evaporated from the interception storage (equation (9)).

$$S_{i,j}^{k+1/2} = S_{i,j}^{k} + PC_i \quad \text{subject to } S_{i,j}^{k+1/2} \le S\max_j \tag{7}$$

$$P_i = PC_i - S_{i,j}^{k+1/2} - S_{i,j}^{k} \tag{8}$$

$$S_{i,j}^{k+1} = S_{i,j}^{k+1/2} - EI_{i,j} \text{ where } EI_{i,j} = \min(\mathrm{EIP}_{i,j}; S_{i,j}^{k+1/2}) \tag{9}$$

where $S_{i,j}$ is the interception storage, $PC_i$ is the precipitation over the vegetation canopy, $P_i$ is the throughfall, or precipitation that gets to the soil surface, $EI_{i,j}$ is the evaporation from the interception storage, $\mathrm{EIP}_{i,j}$ is the potential evaporation from the interception storage, and $k$, $k + 1/2$ and $k + 1$ are related to the start, middle and end of the time step. The value of $\mathrm{EIP}_{i,j}$ is calculated by the Penman-Monteith equation, setting the surface resistance to zero.

First, intercepted water is evaporated at the potential rate $EI_{i,j}$. The remaining fraction of evaporative demand is calculated as (Wigmosta *et al*., 1994):

$$f_{DE} = \frac{(\mathrm{EIP}_{i,j} - EI_{i,j})}{\mathrm{EIP}_{i,j}} \tag{10}$$

and the evapotranspiration of the vegetated soil (soil evaporation plus plant transpiration) is calculated by the Penman-Monteith equation, weighted by the remaining evaporative demand (Wigmosta *et al*., 1994):

$$ET_{i,j} = f_{DE}\left(\frac{\Delta \cdot A + \rho_A \cdot c_p \cdot \frac{D}{r_a}}{\Delta + \gamma\left(1 + \frac{r_s}{r_a}\right)}\right)\frac{M}{\lambda \cdot \rho_W} \tag{11}$$

where $M$ is a constant for unit conversion between m $s^{-1}$ and mm $\Delta t^{-1}$.

Surface resistance is dependent on soil moisture. It is assumed that soil conditions do not restrict evapotranspiration if soil water storage is above a limit given by $W_L = W\mathrm{m}/2$ (Shuttleworth, 1993). In the range between this threshold and the wilting point ($W_{PM}$), surface resistance increases according to equation (12):

$$r_s = r_{j,m}\frac{W_L - W_{PM}}{W_{i,j} - W_{PM}} \tag{12}$$

whilst below the wilting point, $ET_{i,j}$ is zero. In equation (12), the term $r_{j,m}$ is the vegetation-dependent minimum surface resistance, in conditions not affected by soil moisture. This is a parameter related to each GRU, whose value is obtained from the literature and which may have a seasonal variation so that different values are set for each month of the year (m). For simplicity, soil water storage at the wilting point is assumed to be 10% of $W$m.

The remaining terms in the Penman-Monteith equation, such as available energy and aerodynamic resistance, are calculated following Shuttleworth (1993).

The variables $D\mathrm{sup}_{i,j}$, $D\mathrm{int}_{i,j}$ and $D\mathrm{bas}_{i,j}$ in equations (1)–(4) are the surface, interflow and groundwater flow, respectively, generated in the soil layer of the GRU. Since cell dimension is typically large, nearly 10 km in most applications, a flow routing method is needed in order to represent the delay of the inflow to the stream network. As in several other models, linear reservoirs are used to route the flow through the cell. Three independent linear reservoirs are used for each cell, one for each flow generation type: surface, interflow and groundwater. The linear reservoirs collect flow generated in every GRU of the cell, as represented schematically in Fig. 4 for an example of a cell with only two GRUs.

Outflow from these reservoirs is calculated according to the following equations:

$$Q\mathrm{sup}_i = \frac{1}{\mathrm{TKS}_i} \cdot V\mathrm{sup}_i^k \tag{13}$$

$$Q\mathrm{int}_i = \frac{1}{\mathrm{TKI}_i} \cdot V\mathrm{int}_i^k \tag{14}$$

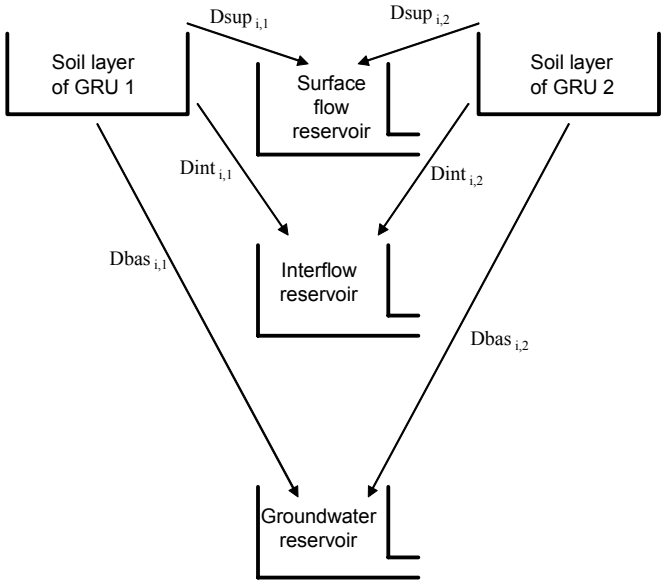


**Fig. 4** Schematic diagram of a cell with two GRUs and the linear reservoirs representing flow routing through the cell to the river network.

$$Q\mathrm{bas}_i = \frac{1}{\mathrm{TKB}_i} \cdot V\mathrm{bas}_i^k \tag{15}$$

where $Q\mathrm{sup}_i$ ($\mathrm{m}^3\ \mathrm{s}^{-1}$) is the outflow of the surface reservoir of cell $i$; $Q\mathrm{int}_i$ ($\mathrm{m}^3\ \mathrm{s}^{-1}$) is the outflow of the subsurface reservoir; $Q\mathrm{bas}_i$ ($\mathrm{m}^3\ \mathrm{s}^{-1}$) is the outflow of the groundwater reservoir; $V\mathrm{sup}_i^k$, $V\mathrm{int}_i^k$ and $V\mathrm{bas}_i^k$ ($\mathrm{m}^3$) are the water volumes in the surface, subsurface and groundwater reservoirs of cell $i$, at time step $k$, already updated by the $D\mathrm{sup}_{i,j}$, $D\mathrm{int}_{i,j}$ and $D\mathrm{bas}_{i,j}$ fluxes drained from the soil layer of each GRU; and $\mathrm{TKS}_i$, $\mathrm{TKI}_i$, $\mathrm{TKB}_i$ (s) are response time parameters.

Following the approach of Ludwig & Bremicker (2006), the parameters TKS and TKI are obtained by the Kirpich formula for time of concentration (equation (16)), which is subsequently corrected by equations (17) and (18):

$$T\mathrm{ind}_i = 3600\left(0.868\frac{L_i^3}{\Delta H_i}\right)^{0.385} \tag{16}$$

$$\mathrm{TKS}_i = C\mathrm{s} \cdot T\mathrm{ind}_i \tag{17}$$

$$\mathrm{TKI}_i = C\mathrm{i} \cdot T\mathrm{ind}_i \tag{18}$$

where $C$s and $C$i are non-dimensional values that correct a first estimate of the retention time of both surface and subsurface flow obtained by equation (18), where $\Delta H$ is estimated by the difference in the maximum and minimum high-resolution digital elevation model (DEM) altitudes in each cell (m), and $L$ is the length of the cell side. Each cell $i$ may have different values for $T$ind, reflecting differences in relief, but the first estimate of the retention time is corrected for surface and subsurface flow during the fitting phase, multiplying it by the non-dimensional parameters $C$s and $C$i, which need to be calibrated. This method for retention time estimates was proposed in

the LARSIM model (Ludwig & Bremicker, 2006), and has the advantage of relating these time parameters to relief for each cell, while at the same time it simplifies calibration. The parameter TKB can be estimated by the recorded hydrograph recession of a long dry period.

Streamflow is routed through the river network using the Muskingum-Cunge method with time steps that can be submultiples of $\Delta t$, and that are adjusted for accuracy according to the stream reach length and slope.

Based on sensitivity analysis (Collischonn, 2001), six parameters were selected for calibration: *W*m, *b*, *K*int, *K*bas, *C*s and *C*i. The parameter *W*m (mm) represents the maximum water storage in the layer of soil, and its value differs for each of the *n* GRUs considered. This parameter is calibrated in order to obtain a good fit between observed and calculated hydrographs; however, it maintains a physical meaning because the range of values within which it is calibrated is set according to the characteristics of root depth of vegetation and soil type. For example, *W*m values for GRUs with forest are sought in a higher range than those for pasture GRUs. Parameters *K*int and *K*bas (mm $\Delta t^{-1}$) are the drainage rates of water from the upper soil layer, when soil is saturated. The parameters are fitted based on recorded hydrographs through trial and error or optimization technique. To obtain the results presented in this paper, only manual calibration was used. Parameters *W*c and *W*z are arbitrarily fixed at 10% of *W*m, which is a reasonable approximation for clayey and sandy-clayey soils (Rawls *et al*., 1993), and are excluded from the calibration procedure.

For the same GRU, parameter values are the same regardless of position within the basin. However, as different cells across the basin have different fractions of land use and vegetation cover classes (grouped in the GRUs), heterogeneity of the basin runoff generation characteristics can be relatively well represented.

Due to the large size of drainage basins within the region, globally-available data sets are used as much as possible. Digital elevation models (DEMs) are now obtained from the Shuttle Radar Topography Mission (SRTM) and for the earlier applications from the Global 30 Arc-Second Elevation data set (GTOPO30). A modified version of the COTAT algorithm by Reed (2003) is used to generate low-resolution drainage networks from high-resolution DEMs (Paz *et al.*, 2006).

Maps of soil type are obtained from sources such as FAO (1988), the Soil and Terrain digital database for Latin America and the Caribbean (SOTERLAC) (FAO, 1998) and the RADAM Brazil mapping database.

Satellite images are classified to obtain vegetation cover and land use for each basin, and climate data are provided by the Brazilian National Water Resources Agency (ANA), NOAA, and Meteorological Aerodrome Report (METAR). The data needed to use the model are combined according to the flowchart in Fig. 5.

The model is run using rainfall and meteorological data from gauging stations within the basin. Values are spatially interpolated at each time step, to the centre of each grid cell, using the inverse-distance-squared weighting method (Burrough & McDonnell, 1998). Some parameters, such as the leaf area index and the surface or canopy resistance used in the rainfall interception and evapotranspiration calculation, are not used in calibration, but are taken from literature, adjusted for seasonal variation where necessary.

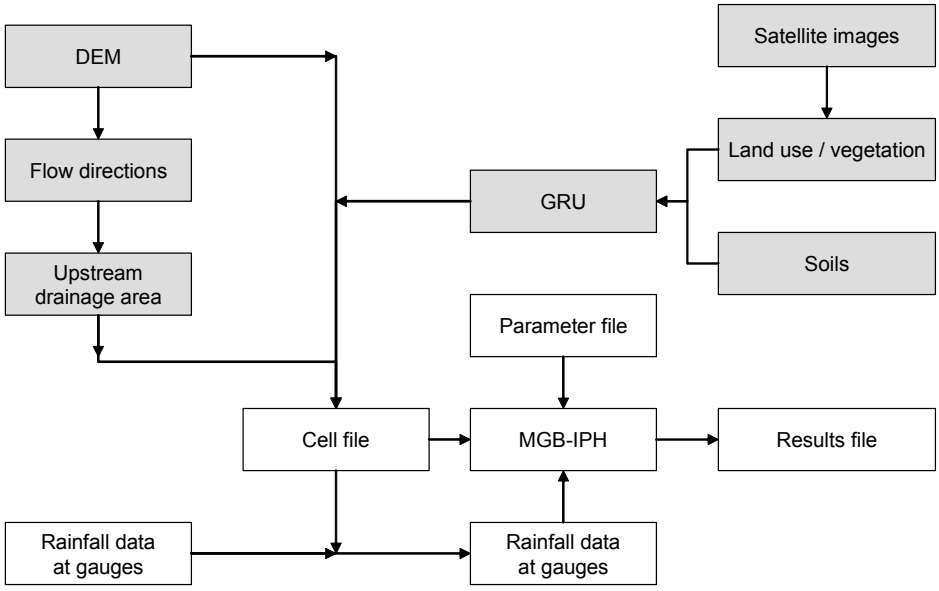


**Fig. 5** Flowchart of data processing and GIS operations in an application of the model (shaded boxes are related to conventional GIS operations).

## MODELLING PROCEDURE

This paper describes application of the model to two basins in southern Brazil which have similar characteristics of soils, vegetation, climate, relief and lithology. The model parameters were calibrated to the conditions of the first basin (the River Taquari-Antas) and were related to land use and vegetation cover. Soil types were not considered in this application because the heterogeneity of soils was relatively low, with shallow soils covering almost all the basin. The same association between land use and vegetation classes and parameter values was then used when the model was applied to the second basin (the River Uruguay). Calculated and observed hydrographs were compared for several gauging stations within the Uruguay basin.

## MODEL FITTING IN THE TAQUARI-ANTAS RIVER BASIN

The Taquari-Antas River basin (26 000 km$^2$) is one of the most important tributaries of the Guaíba-Patos Lagoon system (250 000 km$^2$) in southern Brazil (Fig. 1). The basin is located in a mountainous region between latitudes 28° and 30°S. Soils are very clayey and shallow, and cover a relatively impervious basalt substrate. Relief is pronounced with altitudes varying between 1800 and 20 m, giving rise to highly variable hydrographs and relatively low baseflows. Furthermore, the annual rainfall shows little seasonality, and floods can occur in any month of the year.

Land use and vegetation cover over the basin area are characterised by small farms located mainly in the lower part of the basin. Higher parts are almost completely covered by pasture, with some areas of natural and planted forest. Parts of the original forest still cover steeper slopes along the valleys.

The basin area was divided into 269 square cells, measuring 10 × 10 km$^2$ (Fig. 6(a)). Each cell was further divided into up to four GRUs, according to the land

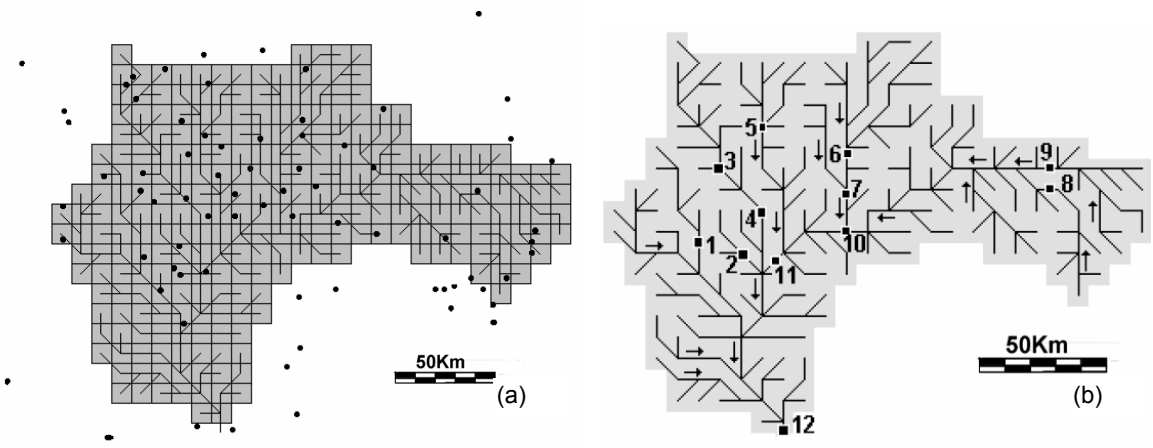


**Fig. 6** Model discretization of the Taquari-Antas River basin showing: (a) raingauge distribution, and (b) streamflow gauges.

**Table 1** Flow gauging stations considered in the Taquari-Antas River basin.

| Number | Name | River | Code | Area (km$^2$) |
|---|---|---|---|---|
| 1 | Passo do Coimbra | Forqueta | 86745000 | 780 |
| 2 | Ponte do Jacaré | Jacaré | 86700000 | 432 |
| 3 | Linha Colombo | Guaporé | 86560000 | 1 980 |
| 4 | Santa Lúcia | Guaporé | 86580000 | 2 382 |
| 5 | Passo Migliavaca | Carreiro | 86480000 | 1 250 |
| 6 | Passo Guaiaveira | Turvo | 86410000 | 2 839 |
| 7 | Passo do Prata | Prata | 86440000 | 3 622 |
| 8 | Passo Tainhas | Tainhas | 86160000 | 1 107 |
| 9 | Passo do Gabriel | Antas | 86100000 | 1 725 |
| 10 | Ponte Rio das Antas | Antas | 86470000 | 12 298 |
| 11 | Muçum | Taquari | 86510000 | 15 826 |

use and vegetation cover, classified from LANDSAT TM images (water, pasture, forest and agriculture). River characteristics, such as length and slope were obtained manually from 1:250 000 topographic maps. A digital elevation model (DEM) of the region was obtained from the GTOPO30 data set.

Rainfall records were available from 72 gauges, only 50 of which are inside the basin, many with long periods of missing data (Fig. 3(a)). Eleven flow gauge stations ranging from 463 to 15 826 km$^2$ (Fig 6(b)) were selected. Table 1 shows some characteristics of the gauging stations considered. Point 12 in Fig. 6(b) is the outlet of the basin where there is no gauging station. Rainfall and streamflow data from 1970 to 1980 were split into two parts. The period 1970–1975 was used for calibration, and 1976–1980 for verification.

Parameters were calibrated manually by trial and error using both visual inspection of calculated and recorded hydrographs and the following statistical measures: the Nash-Sutcliffe model efficiency coefficient (NS, equation (19)), the Nash-Sutcliffe coefficient for logarithms of discharge values ($NS_{log}$, equation (20)) and relative streamflow volume error ($\Delta V$, equation (21)):

$$\mathrm{NS} = 1 - \frac{\sum \left(Q_{\mathrm{obs}}(t) - Q_{\mathrm{cal}}(t)\right)^2}{\sum \left(Q_{\mathrm{obs}}(t) - \overline{Q_{\mathrm{obs}}}\right)^2} \tag{19}$$

$$\mathrm{NS}_{\log} = 1 - \frac{\sum \left(\ln\left(Q_{\mathrm{obs}}(t)\right) - \ln\left(Q_{\mathrm{cal}}(t)\right)\right)^2}{\sum \left(\ln\left(Q_{\mathrm{obs}}(t)\right) - \overline{\ln\left(Q_{\mathrm{obs}}\right)}\right)^2} \tag{20}$$

$$\Delta V = \frac{\sum \left(Q_{\mathrm{cal}}(t)\right) - \sum \left(Q_{\mathrm{obs}}(t)\right)}{\sum \left(Q_{\mathrm{obs}}(t)\right)} \tag{21}$$

The calibration procedure considered mainly the results at the Muçum gauging station (see Table 3), where the basin size is approximately 15 000 km$^2$. This point was chosen because it has the largest drainage area and because its basin encompasses the locations of five other gauging stations (see Fig. 6(b)). Moreover, the streamflow record of this gauging station had fewer missing data. At this station the best values of the objective functions NS, $\mathrm{NS}_{\log}$ and $\Delta V$ were sought, while the results were also monitored by visual comparison of observed and calculated hydrographs. Results at other gauging stations were used to verify the calibration.

During the calibration, values of *W*m for forest were sought in a range somewhat higher than that of *W*m for pasture and agriculture, in order to reflect the differences in root depth, which is normally higher for forests than for pasture or crops (Kleidon & Heimann, 1999). Values for fitted parameters in the Taquari-Antas basin are presented in Table 2. The relatively small difference between calibrated *W*m for forest (200 mm) and for pasture (150 mm) may be due to the very shallow soils found in the basin, particularly in the regions with bigger slope, where the remaining forests are concentrated.

Figure 7 shows observed and calculated daily streamflow at the Muçum gauging station, from June to December 1973, and Fig. 8 shows results for the Passo Migliavaca gauging station, from June to October 1972. These figures show that there was a relatively good agreement between the hydrographs. The model tended to underestimate peak flows, but this was somewhat neglected because rating curves are not well defined at high flows, due to very few discharge measurements being available at higher stages (Collischonn & Tucci, 2001). Attempting to calibrate the model by fitting to peak flows would require excessive reliance on very questionable data.

**Table 2** Values of the model parameters calibrated in the Taquari-Antas River basin.

| Parameter | Value | Unit |
|---|---|---|
| W*m* | 200 – forest<br>150 – pasture<br>100 – agriculture<br>0 – water | mm |
| *b* | 0.1 | - |
| *K*int | 7.2 | mm d$^{-1}$ |
| *K*bas | 0.50 | mm d$^{-1}$ |
| *W*c | 0.1 × *W*m | mm |
| *C*s | 14 | - |
| *C*i | 90 | - |
| TKB | 25 | d |

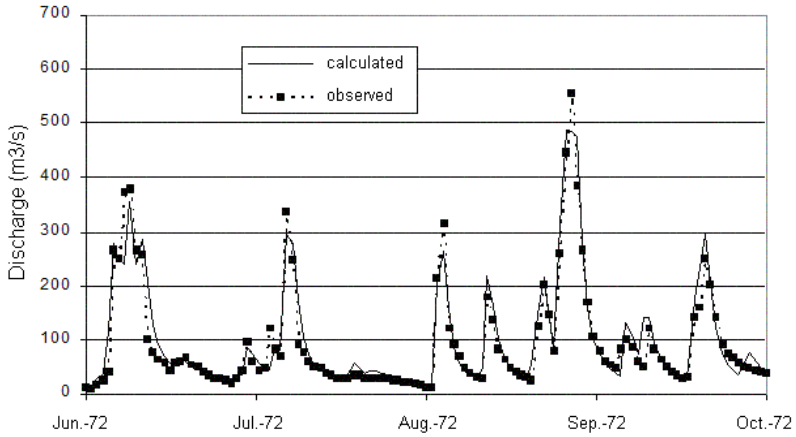


**Fig. 7** Calculated and observed hydrographs of the Taquari-Antas River at the Muçum gauging station (15 826 km$^2$).

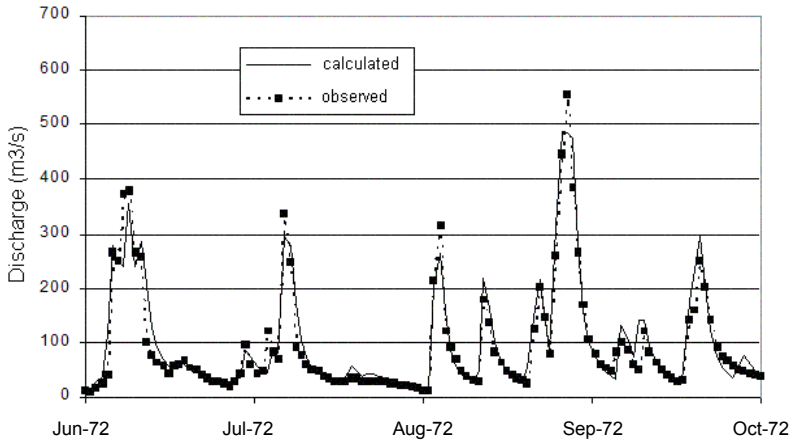


**Fig. 8** Calculated and observed hydrographs of the Carreiro River, one of the main tributaries of the Taquari-Antas, at the Passo Migliavaca gauging station (1250 km$^2$).

The ability of the model to generate streamflow time series at interior points of the basin was also tested by comparing results at several gauging stations within it (Table 3). Values found for the objective functions, and visual inspection of Fig. 8, suggest that the model can be used to estimate streamflow at ungauged points of this basin.

Table 3 shows that results tend to be better when evaluated at gauging stations controlling larger drainage areas. This tendency can be expected because the model structure was proposed for applications at large basins and because the heterogeneity of small basins cannot be adequately described by the grid cell size adopted for the Taquari-Antas River basin (10 × 10 km$^2$). Differences in performance between calibration and verification periods are relatively small for some basins, and results may be even better during the verification period for others, although for the two stations with the largest drainage area (Ponte Rio das Antas and Muçum) there is a relatively strong decrease in performance as measured by the Nash-Sutcliffe efficiency.

Table 3 also shows that model performance at internal points was relatively good, and did not decrease abruptly from the calibration to the verification period. The last

**Table 3** Summary of results of model calibration in the Taquari-Antas basin.

| River | Gauging station | Calibration (1970–1975): | | | Verification (1976–1980): | | |
|---|---|---|---|---|---|---|---|
| | | NS | $NS_{log}$ | $\Delta V$ (%) | NS | $NS_{log}$ | $\Delta V$ (%) |
| Forqueta | Passo Coimbra | 0.66 | 0.73 | –4.11 | 0.77 | 0.77 | –1.14 |
| Jacaré | Passo Jacaré | 0.68 | 0.71 | –2.54 | 0.68 | 0.75 | –4.52 |
| Guaporé | Linha Colombo | 0.80 | 0.79 | –1.18 | 0.81 | 0.84 | –2.69 |
| Guaporé | Santa Lúcia | 0.87 | 0.85 | 1.62 | 0.79 | 0.82 | –2.51 |
| Carreiro | Passo Migliavaca | 0.86 | 0.85 | 1.15 | 0.69 | 0.84 | –3.84 |
| Turvo | Passo Barra Guaiaveira | 0.83 | 0.81 | 3.07 | 0.81 | 0.86 | 1.43 |
| Prata | Passo do Prata | 0.85 | 0.85 | 3.48 | 0.84 | 0.85 | –2.49 |
| Tainhas | Passo Tainhas | 0.82 | 0.81 | 4.89 | 0.80 | 0.79 | 1.31 |
| Antas | Passo do Gabriel | 0.76 | 0.82 | –5.10 | 0.40 | 0.76 | 5.71 |
| Antas | Ponte Rio das Antas | 0.90 | 0.85 | –1.11 | 0.83 | 0.81 | –6.07 |
| Taquari | Muçum | 0.90 | 0.86 | 1.24 | 0.82 | 0.84 | –1.01 |

NS: Nash-Sutcliffe efficiency of daily discharge; $NS_{log}$: Nash-Sutcliffe efficiency of logarithms of daily discharge; $\Delta V$: difference between runoff volumes.

seven gauging stations presented in Table 3 are located inside the drainage basin of the Muçum gauging station, and it can be seen that the model efficiencies (NS and $NS_{log}$) are more or less the same in both periods, at least for the rivers Turvo, Prata and Tainhas. The exceptions are the River Antas at Passo do Gabriel, where the NS efficiency fell from 0.76 to 0.40, and the River Carreiro at Passo Migliavaca, where NS fell from 0.86 to 0.69. In the case of the gauge at Passo do Gabriel, this may be related to the poor raingauge coverage of this relatively small basin (see point 9 in Fig 6(b)).

Floods along the Taquari-Antas River and its tributaries are very rapid, since the basin response is dominated by surface runoff. As shown in Fig. 7, the discharge of the Taquari-Antas can rise from 500 to 4000 $m^3 s^{-1}$ in a day. Such large variations limited the quality of the results since, because of the limited availability of data, the model could not use time steps shorter than one day.

## PARAMETER TRANSFERABILITY TEST TO THE UPPER URUGUAY BASIN

The River Uruguay is one of the main tributaries of La Plata basin. Its upper basin lies in Brazil where the river flows east–west. In its middle course the river flows south, defining the border between Brazil and Argentina. The lower course of the river forms the frontier between Uruguay and Argentina up to where the river joins the Paraná River, forming the Plata River. The upper part of the Uruguay basin lies exclusively in Brazil with a total drainage area of 75 000 $km^2$ (Fig. 1).

As in the nearby Taquari-Antas River basin, land use and vegetation cover consist mainly of small farms, with some forest remaining on the steeper slopes. Some areas of reforestation and pasture are found in headwater areas of the basin.

The Uruguay River basin was represented by 681 cells of 0.1 × 0.1 degrees. Land-use data were obtained from classified NOAA AVHRR images (grid size of 1 km), resulting in five classes: forest; pasture; agriculture; mixed forest and pasture; mixed forest and agriculture. Low spatial resolution of the NOAA AVHRR images did not

**Table 4** Values of the model parameters used in the Uruguay River basin.

| Parameter | Value | Unit |
|---|---|---|
| *W*m | 200 – forest<br>200 – mixed forest and pasture<br>200 – mixed forest and agriculture<br>150 – pasture<br>100 – agriculture | mm |
| *b* | 0.1 | - |
| *K*int | 7.2 | mm $d^{-1}$ |
| *K*bas | 0.50 | mm $d^{-1}$ |
| *W*c | 0.1 × *W*m | mm |
| *C*s | 14 | - |
| *C*i | 90 | - |
| TKB | 25 | d |

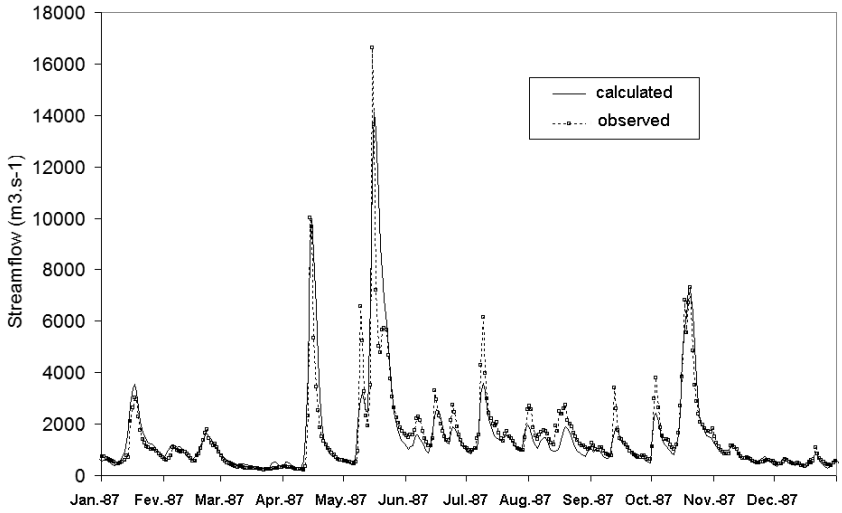


**Fig. 9** Calculated and observed hydrographs of the river Uruguay at the Passo Caxambu gauging station (52 671 $km^2$) with parameters transferred from the Taquari-Antas basin.

allow classification into entirely separate classes, and some parts of the basin were allocated to mixed classes. Parameter values for each GRU were fixed at the same values obtained in the Taquari-Antas basin (Table 4). The differences between Table 2 and Table 4 are due to the values for the classes of mixed land use and land cover, which were not found in the Taquari-Antas River basin. For simplicity, and by local knowledge of land cover and vegetation, the *W*m parameter was fixed at 200 mm for the two mixed classes, since both have relatively large quantities of forest.

The model was applied using data from 1985–1995. Observed and calculated hydrographs for 1987 at the Passo Caxambu (basin area 52 671 $km^2$) are shown in Fig. 9. Values of the objective functions at five gauging stations located on the River Uruguay and some tributaries are presented in Table 5. Figure 9 shows that some minor peaks during the austral winter of 1987 were underestimated, but most of the larger peaks were well reproduced. It can be seen (Table 5) that the best statistical results were obtained for larger basins, with Nash-Sutcliffe efficiencies up to 0.84, and

**Table 5** Summary of results of the hydrological model application without calibration of the parameters at five gauging stations in the Uruguay basin.

| Station | River | Basin area ($km^2$) | NS | $NS_{log}$ | $\Delta V$ (%) |
|---|---|---|---|---|---|
| Passo Caru | Canoas | 9 868 | 0.62 | 0.67 | –21.7 |
| Marcelino Ramos | Uruguay | 41 267 | 0.79 | 0.80 | –3.4 |
| Passo Caxambu | Uruguay | 52 671 | 0.84 | 0.83 | –7.4 |
| Barra do Chapecó | Chapecó | 8 267 | 0.76 | 0.73 | –11.9 |
| Passo Rio da Várzea | Da Várzea | 5 356 | 0.76 | 0.75 | –16.9 |

NS: Nash-Sutcliffe efficiency of daily discharge; $NS_{log}$: Nash-Sutcliffe efficiency for logarithms of daily discharge; $\Delta V$: total runoff volume error.

relative volume errors below 10%. When evaluating the quality of these results it must be remembered that the model was not calibrated for this basin.

Simulated mean discharges were below those recorded at all gauging stations, as can be seen by negative relative volume errors. This may be a consequence of the relative high value (200 mm) given to the parameter *W*m for classes that are mixed forest and pasture or forest and agriculture. A lower value of this parameter would result in less calculated soil storage and less calculated evapotranspiration, resulting in larger values of calculated mean discharge. A more reasonable value for the parameter *W*m would be 175 mm for the pasture/forest mix and 150 for the agriculture/forest mix, if we consider the mixture to be exactly the mean of the original values.

After this first application without calibration, the model was also fitted in this basin, and was then used to forecast streamflow of the River Uruguay up to 5 months in advance, driven by forecasts of rainfall from seasonal climatic predictions of the global model of the Brazilian Centre of Weather and Climate Prediction (Tucci *et al.*, 2003).

## CONCLUSIONS

This paper presents a description of the large-scale hydrological model MGB-IPH, which is being used in several applications in basins covering areas from 3000 to nearly 1 000 000 $km^2$ in South America. The model was specially designed to be used in large basins with relatively scarce data, using globally available data as far as possible. Following the method adopted in several other large-scale hydrological models, parameter values are associated to classes of soil, land use and vegetation cover and to the characteristics of relief, using the hydrological response unit (HRU) or grouped response unit (GRU) approach. The model was used to test whether associations could be established that relate readily available data to model parameter values by a proxy-basin test, using data of two basins with similar characteristics in southern Brazil.

The model was firstly applied to the Taquari-Antas River basin where it was manually calibrated to one gauging station, and was verified at another ten gauges. The model was then applied to the Upper Uruguay River basin without parameter calibration, assuming that the same relation found between land use/vegetation cover and parameter values in the Taquari-Antas River basin could be assumed to be valid for the Uruguay River basin.

Results in the Taquari-Antas River basin showed a tendency to be better at streamgauges draining larger river basins. Nevertheless, model performance at internal points was relatively good, and did not decrease abruptly from the calibration to the verification period.

Calculated and observed streamflow results in the Uruguay basin are in good agreement for gauges with drainage area ranging from 5356 to 52 671 km$^2$, although relatively large total water yield errors were found for three tributaries.

Overall results suggest that the model would present reasonable predictions in ungauged basins if parameters can be fitted in a basin with similar characteristics. This result is valid for the conditions found in southern Brazil, where surface runoff dominates the hydrograph due to the shallow and impermeable soils.

**Acknowledgements** The authors acknowledge with gratitude the support of the Brazilian National Electricity Agency (ANEEL), and the Brazilian Scientific Councils CNPq and CAPES. Suggestions proposed by R. T. Clarke were also greatly appreciated.

## REFERENCES

Allasia, D. G., Silva, B., Collischonn, W. & Tucci, C. E. M. (2006) Large basin simulation experience in South America. In: *Prediction in Ungauged Basins: Promises and Progress* (ed. by M. Sivapalan, T. Wagener, S. Uhlenbrook, E. Zehe, V. Lakshmi, Xu Liang, Y. Tachikawa & P. Kumar) (Proc. Brazil Symp., April 2005), 360–370. IAHS Publ. 303. IAHS Press, Wallingford, UK.

Andersen, J., Refsgaard, J. C. & Jensen, K. H. (2001) Distributed hydrological modelling of the Senegal River Basin—model construction and validation. *J. Hydrol.* **247**, 200–214.

Beven, K. (2001a) How far can we go in distributed hydrological modelling? *Hydrol. Earth System Sci.* **5**(1), 1–12.

Beven, K. (2001b) *Rainfall–Runoff Modelling: The Primer.* Wiley, Chichester, UK.

Bremicker, M.; Homagk, P. & Ludwig, K. (2004) Operational low-flow-forecast for the Neckar river basin (in German). *Wasserwirtschaft* **7/8**, 40–46.

Burrough, P. A. & McDonnell, R. A. (1998) *Principles of Geographical Information Systems*. Oxford University Press, USA.

Collischonn, W. (2001) Hydrologic simulation of large basins (in Portuguese), PhD Thesis, Inst. de Pesqui. Hidraul., Univ. Fed. do Rio Grande do Sul, Porto Alegre, Brazil.

Collischonn, W. & Tucci, C. E. M. (2001) Hydrological simulation of large drainage basins (in Portuguese). *Brazilian J. Water Resour.* **6**(1), 15–35.

Evans, J. P. (2003) Improving the characteristics of streamflow modelled by regional climate models. *J. Hydrol.* **284**, 211–227.

FAO (Food and Agriculture Organization) (1988) *Soil Map of the World*. Revised legend. Reprinted with corrections. World Soil Resources Report no. 60. FAO, Rome, Italy.

FAO (Food and Agriculture Organization) (1998) *Soil and Terrain Database for Latin America and the Caribbean* (1:5 million scale). (CD-ROM). FAO Land and Water Digital Media Series no. 05, FAO, Rome, Italy.

Guo, S., Wang, J., Xiong, L., Aiwen Y. & Li, D. (2002) A macro-scale and semi-distributed monthly water balance model to predict climate change impacts in China. *J. Hydrol*. **268**, 1–15.

Habets, F., Etchevers, P., Golaz, C., Leblois, E., Ledoux, E., Martin, E., Noilhan, J. & Ottlé, C. (1999) Simulation of the water budget and the river flows of the Rhone basin. *J. Geophys. Res.***104**(24), 31145–31172.

Kite, G. W. & Kouwen, N. (1992) Watershed modeling using land classifications. *Water Resour. Res.* **28**(12), 3193–3200.

Klemes, V. (1986) Operational testing of hydrological simulation models. *Hydrol. Sci. J.* **31**(1), 13–24.

Kleidon, A. & Heimann, M. (1999) Deep-rooted vegetation, Amazonian deforestation, and climate: results from a modelling study. *Global Ecol. and Biogeogr.* **8**, 397–405.

Kouwen, N. & Mousavi, S. F. (2002) WATFLOOD/SPL9: Hydrological model and flood forecasting system. In: *Mathematical Models of Large Watershed Hydrology* (ed. by V. P. Singh & D. K. Frevert). Water Resources Publications. Highlands Ranch. Colorado, USA.

Kouwen, N., Soulis, E. D., Pietroniro, A., Donald, J. & Harrington, R. A. (1993) Grouped response units for distributed hydrologic modeling. *J. Water Resour. Plann. Manage.* **119**(3), 289–305.

Krysanova, V.; Müller-Wohlfeil, D.-I. & Becker, A. (1998) Development and test of a spatially distributed hydrological/water quality model for mesoscale watersheds. *Ecol. Modelling* **106**, 261–289.

Liang, X., Lettenmaier, D. P., Wood, E. F. & Burges, S. J. (1994) A simple hydrologically based model of land surface water and energy fluxes for general circulation models. *J. Geophys. Res.* **99**(7), 14415–14428.

Ludwig, K. & Bremicker, M. (eds) (2006) The water balance model LARSIM—design, content and applications. *Freiburger Schriften zur Hydrologie* **22**. Institut für Hydrologie Universität Freiburg, Germany.

Matheussen, B., Kirschbaum, R. L., Goodman, I. A., O'Donnell, G. M. & Lettenmaier, D. P. (2000) Effects of land cover change on streamflow in the interior Columbia River basin (USA and Canada). *Hydrol. Processes* **14**, 867–885.

Nijssem, B, Lettenmaier, D. P., Liang, X., Wetzel, S. W. & Wood, E. F. (1997) Streamflow simulation for continental-scale river basins. *Water Resour. Res.* **33**(4), 711–724.

Paz, A. R., Collischonn, W. & Silveira, A. L. L. (2006) Improvements in large scale drainage networks derived from digital elevation models. *Water Resources Res.* **42**(8), W08502, doi:10.1029/2005WR004544.

Rawls, W. J., Ahuja, L. R., Brakensiek, D. & Shirmohammadi, A. (1993) Infiltration and soil water movement. In: *Handbook of Hydrology* (ed. by D. Maidment), 5.1–5.51. McGraw-Hill, New York, USA.

Reed, S. M. (2003) Deriving flow directions for coarse-resolution (1–4 km) gridded hydrologic modeling. *Water Resour. Res*. **39**(9), 1238.

Refsgaard, J. C. & Storm, B. (1995) MIKE SHE. In: *Computer Models of Watershed Hydrology* (ed. by V. P. Singh), 809–846. Water Resources Publications, Littleton, Colorado, USA.

Ribeiro A., Vieira da Silva, R., Collischonn, W. & Tucci, C. E. M. (2005) Hydrological modelling in Amazonia—use of the MGB-IPH model and alternative data base. In: *Prediction in Ungauged Basins: Promises and Progress* (ed. by M. Sivapalan, T. Wagener, S. Uhlenbrook, E. Zehe, V. Lakshmi, Xu Liang, Y. Tachikawa & P. Kumar) (Proc.. Foz do Iguaçu Symp., 2006), 246–254. IAHS Publ. 303, IAHS Press, Wallingford, UK.

Sausen, R., Schubert, S. & Dümenil, L. (1994) A model for river runoff for use in coupled atmosphere–ocean models. *J. Hydrol*. **155**, 337–352.

Shuttleworth, W. .J. (1993) Evaporation. In: *Handbook of Hydrology* (ed. by D. Maidment), 4.1–4.53 McGraw-Hill, New York, USA.

Singh, V. P. & Frevert, D. K. (eds) (2002) *Mathematical Models of Large Watershed Hydrology*. Water Resources Publications. Highlands Ranch, Colorado, USA.

Sivapalan, M., Takeuchi, K., Franks, S. W., Gupta, V. K., Karambiri, H., Lakshmi, V., Liang, X., McDonnell, J. J., Mendiondo, E. M., O'Connell, P. E., Oki, T., Pomeroy, J. W., Schertzer, D., Uhlenbrook, S. & Zehe, E. (2003) IAHS Decade on Prediction in Ungauged Basins (PUB), 2003–2012: Shaping an exciting future for the hydrological sciences. *Hydrol. Sci. J.* **48**(6), 857–880.

Soulis, E. D., Kouwen, N., Pietroniro, A., Seglenieks, F. R., Snelgrove, K. R., Pellerin, P., Shaw, D. W. & Martz, L. W. (2004) A framework for hydrological modelling in MAGS. In: *Prediction in Ungauged Basins: Approaches for Canada's Cold Regions* (ed. by C. Spence, J. W. Pomeroy & A. Pietroniro). CWRA ACRH Press, Ontario, Canada.

Todini, E. (1996) The ARNO rainfall–runoff model. *J. Hydrol.* **175**, 293–338.

Tucci, C. E. M., Marengo, J. A., Silva Dias, P. L., Collischonn, W., Silva, B. C., Clarke, R. T., Cardoso, A. O., Juarez, R. N., Sampaio, G., Chan, C. S. & Tomasella, J. (2005) Streamflow forecasting in São Francisco River basin based on climatic forecasting. *Technical Report ANEEL/WMO/98/00*. Porto Alegre, Brazil (in Portuguese).

Tucci, C. E. M., Clarke, R. T., Collischonn, W., Dias, P. L. S. & Sampaio, G. (2003) Long term flow forecast based on climate and hydrological modeling: Uruguay River basin. *Water Resour. Res.* **39**(7), 1181, doi:10.1029/2003WR002074.

Ubarana, V. N. (1996) Observation and modelling of rainfall interception loss in two experimental sites in Amazonian forest. In: *Amazonian Deforestation and Climate* (ed. by J. H. C. Gash, C. A. Nobre, J. M. Roberts & R. L. Victoria), 151–162. John Wiley & Sons, Chichester, UK.

Wigmosta, M. S., Vail, L. W. & Lettenmaier, D. P. (1994) A distributed hydrology–vegetation model for complex terrain. *Water Resour. Res.* **30**(6), 1665–1679.

Wood, E. F., Lettenmaier, D. P. & Zartarian, V. G. (1992) A land surface hydrology parameterization with subgrid variability for general circulation models. *J. Geophys. Res*. **97**(3), 2717–2728.

Zhao, R. J., Zuang, Y. L., Fang, L. R., Liu, X. R. & Zhang, Q. S. (1980) The Xinanjiang model. In: *Hydrological Forecasting* (Proc. Oxford Symp., April 1980), 351–356. IAHS Publ. 129, IAHS Press, Wallingford, UK.

**Received 6 June 2006; accepted 2 May 2007**